# 30-512 MHz Hybrid Power Amplifier Design Using GaN transistor

**S. Pisa\*, S. Chicarella\*, R. Cusani\*, C. Jerome°**

\* Department of Information Engineering, Electronics and Telecommunications, Sapienza University of Rome, 00184 Rome Italy

° Polyfet RF Devices, 1110 Avenida Acaso Camarillo, Ca. 93012

**ABSTRACT:** In this paper, using a GaN transistor, a class AB single-ended power amplifier with 30-512 MHz frequency band and 100 W saturated output power has been designed and implemented. An electromagnetic and a thermal CAD by CST have been employed to design the amplifier matching networks and the heat removal assembly, respectively. For 30 dBm input power, the measured gain is 19 dB +/- 1 dB, the average PAE is 61% and the return loss is always better than -7.5 dB. The measured responses are state of art results and are in good agreement with simulations performed with a circuital CAD by NI AWR.

# I. INTRODUCTION

High Power amplifiers (HPA) are the costly part of radio communication systems so that accurate design is recommended [1], [2]. In particular, HPA operating in the 30 MHz-512 MHz band are employed for mobile radio communications, radio and television broadcasting, air traffic control, marine communications, weather forecasting systems [3], [4]. For these applications, a significant cost reduction is achieved if a single broadband amplifier is used. To this end, GaN HEMT devices are of interest because of their high breakdown voltage, saturation velocity and permittivity. This leads to higher powers for a given device area with respect to other technologies. Moreover, the parasitic capacitances are small enough to maintain these properties at high frequencies [5]-[7].

In radio-communication systems, the efficiency of the power amplifier is a fundamental requirement. High efficiency means reduced lost power and hence "greener" amplifiers. Moreover, a high efficiency reduces the power consumption of the cooling system necessary to remove the dissipated energy [4].

In this paper, using a GaN transistor, a high efficiency 30-512 MHz HPA with 100 W output power is designed and implemented. Its block model is shown in Fig.1. Among the various blocks, the transistor, the matching networks and the heat removal are particularly critical and will be discussed in more detail in the next paragraphs.
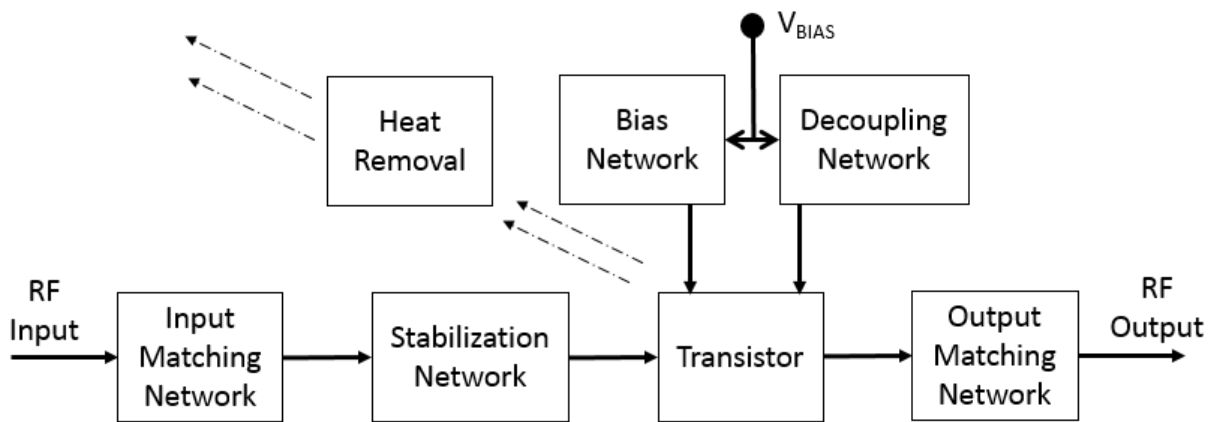


Figure 1: Block model of the considered power amplifier

## II. OPTIMISED TRANSISTOR MODEL

In this design, the GX3442 GaN HEMT by Polyfet has been used [8]. For this transistor a model constituted by two CURTICE FET [9] is available in the microwave office element libraries. The model parameter VTO and BETA of the CURTICE model have been optimized to give a current Ids $\cong$ 17 A with Vgs = 2 V and Ids $\cong$ 400 mA with Vgs = -2.15 V as reported in the transistor specifications [8], [10]. The optimized values for the two transistors of the GX3442 model are VTO1=-2.53, BETA1=3.8, VTO2=-5, BETA2=35. Fig. 2 shows the achieved transistor trans-characteristic achieved with the microwave office (MWO) by NI AWR circuital CAD.
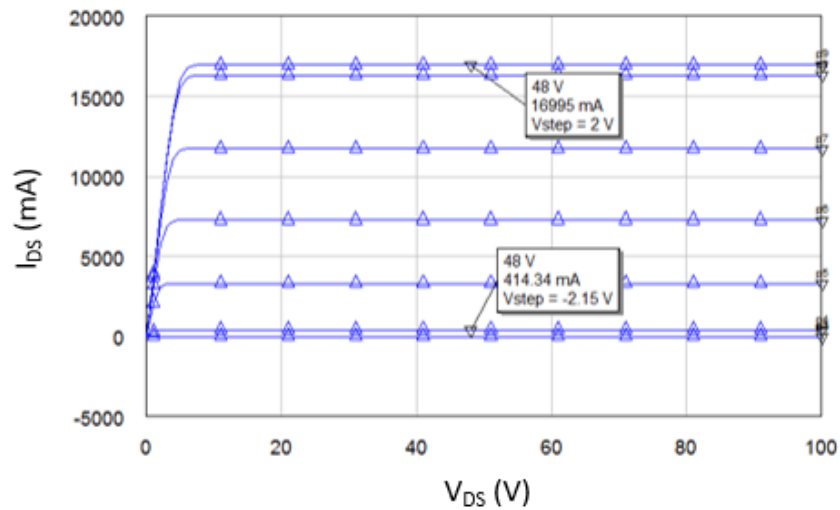


Figure 2: Trans-characteristic of the optimized GX3442 GaN

## III. COAXIAL TRANSFORMERS MODELING

Wideband matching network for RF power amplifiers have been theoretically studied in the past and many schematic and design equations have been reported [11]-[13]. Here, the coaxial transformer used as matching network for the amplifier has been numerically simulated inside the electromagnetic CAD Microwave Studio by CST, by using the FEM solver (see Fig. 3). Fig. 4 shows the transformer implemented by using binocular ferrite 61 by Amidon with relative permeability equal to 125.
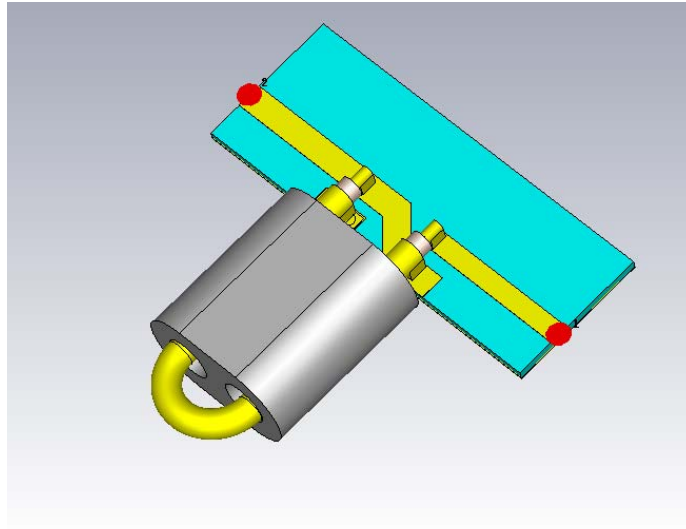
Figure 3: Coaxial transformer simulated inside the CAD Microwave studio by CST
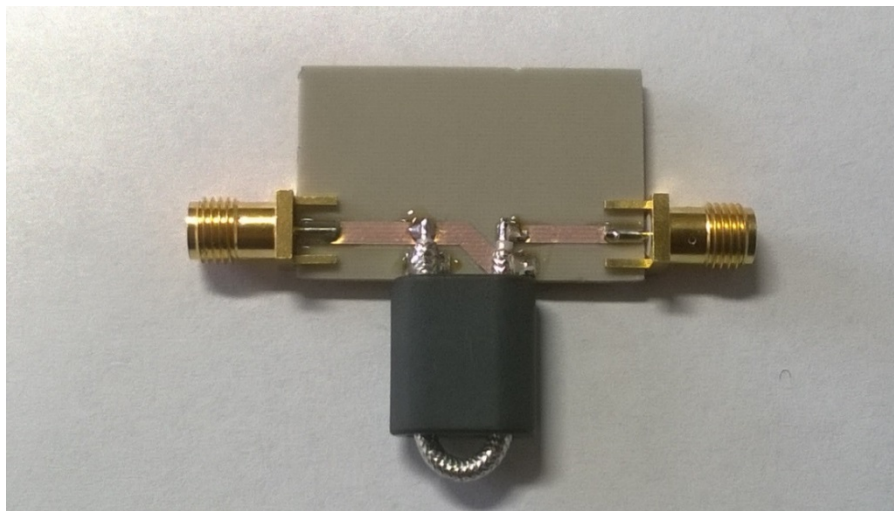


Figure 4: Transformer realization by using binocular ferrite 61 by Amidon

The typical frequency behavior of ferrite 61 has been interpolated with the Debye model [14] with $f_c=40\cdot10^6$ Hz:

$$\mu_r^c = \frac{\mu_r}{1+j\frac{f}{f_c}} = \frac{\mu_r}{1+\left(\frac{f}{f_c}\right)^2} - \frac{j\mu_r\frac{f}{f_c}}{1+\left(\frac{f}{f_c}\right)^2} = \mu_r' - j\,\mu_r'' \tag{1}$$

Finally, the transformer has been implemented inside the circuital CAD Microwave office (see Fig. 5).
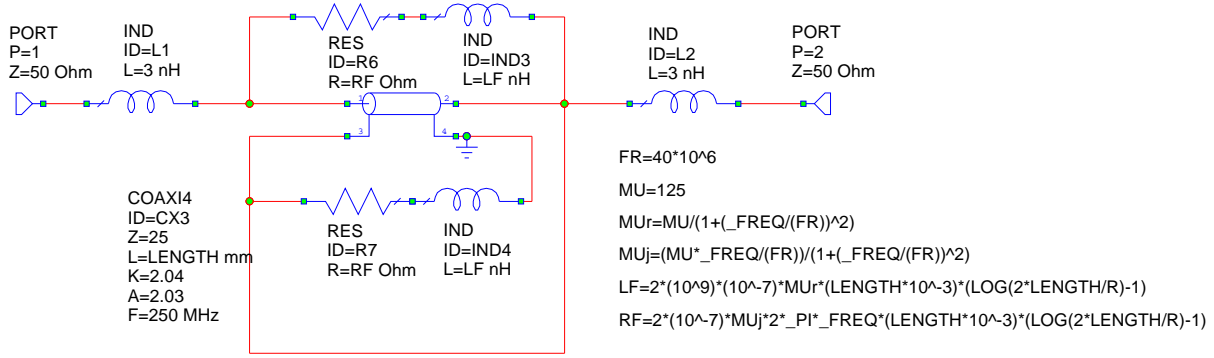
Figure 5: Transformer implementation in the CAD microwave office by NI-AWR

This circuit model takes into account the presence of the binocular ferrite modeled with the series of an inductance (*LF*) and a resistance (*RF*) related to the real and imaginary part of the relative permeability of the ferrite, respectively. In particular, *LF* and *RF* expressions are:

$$LF = \mu_r' \, 2 \, 10^{-7} \, l \, \left[ ln\left(\frac{2l}{r}\right) - 1 \right] \tag{2}$$

$$RF = \mu_r'' \, \omega \, 2 \, 10^{-7} \, l \, \left[ ln\left(\frac{2l}{r}\right) - 1 \right] \tag{3}$$

In the circuit model two series inductor (L1 and L2) have been added to simulate the presence of wires between the component ports and the coaxial cable.

Fig. 6 shows a comparison among the $S_{21}$ parameter of the coaxial transformer, evaluated with the CST model, the MWO circuit, and measured on the realized transformer of Fig. 4. In particular, the presence of a 3 nH inductance at the input and output terminals allows for a better agreement between MWO simulations and measurements.
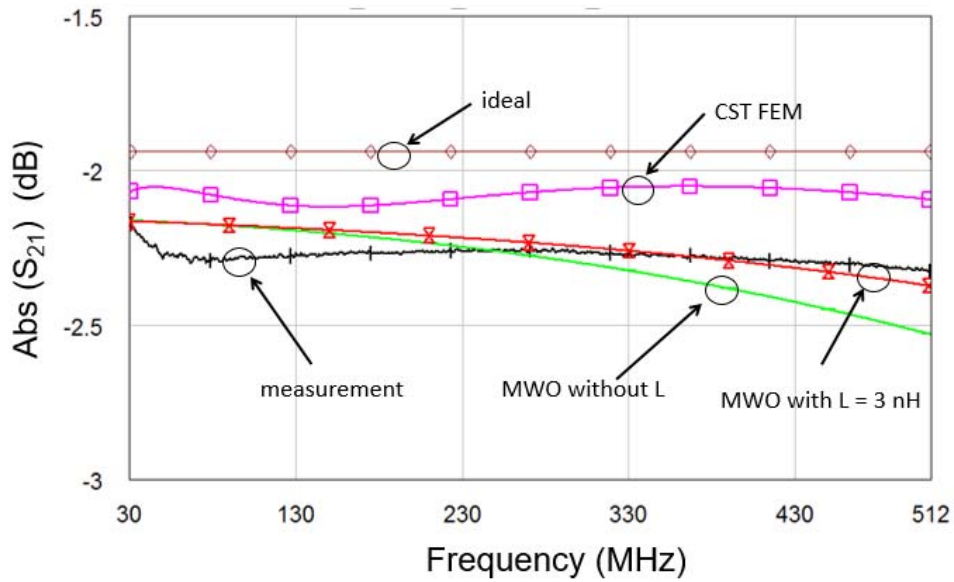
Figure 6: Abs($S_{21}$) of the coaxial transformer as a function of frequency. Comparison among simulations with CST, MWO model, and measurements on the realized transformer

## IV. POWER AMPLIFIER THERMAL MODELING

The mechanical structure hosting the amplifier board and dissipating the heating produced by the transistor has been designed as in Fig. 7.
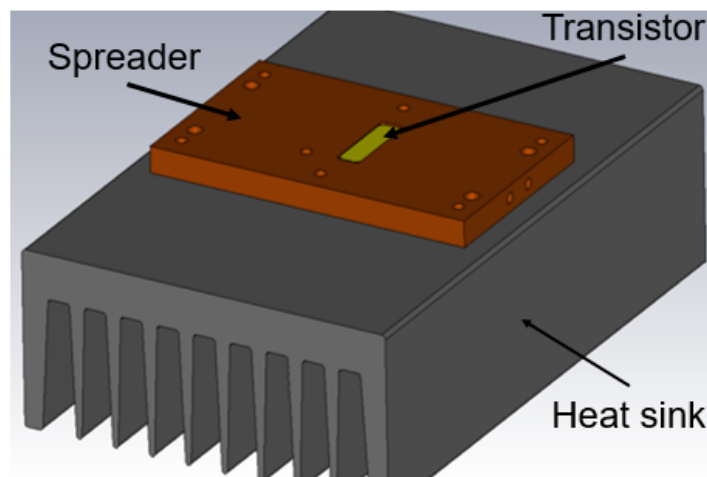


Figure 7: Spreader and heat sink structure

**6**

When a power "P" is dissipated inside the transistor, the temperature variation between the transistor junction ($T_j$) and the air ($T_a$) is given by:

$$\Delta T = T_j - T_a = P * (R_{jc} + R_{sh} + R_{ha}) \tag{4}$$

where $R_{jc}$ is the junction-to-case thermal resistance, $R_{sh}$ the spreader to heat sink thermal resistance and $R_{ha}$ is the heat sink to air thermal resistance.

For the $R_{jc}$ parameter of the GX3442 transistor, a value of 1.9 °C/W is given by the factory [8]. In order to estimate the other two thermal resistances, the spreader and heat sink thermal responses have been simulated inside the CAD Microwave studio by CST (see Fig. 7). CST implements a finite difference solution of Fourier equation [15]-[17]. A 50 W thermal source has been impressed in the transistor flange. At the ventilated and non-ventilated surfaces, convective coefficients of 30 W/m$^2$K and 5 W/m$^2$K have been imposed, respectively [18]. Fig. 8 shows the thermal simulation result. The maximum thermal variation at the flange is about 24 °C hence from (4) it is: $R_{sh} + R_{ha} \approx 0.48$. In conclusion, the expected transistor temperature increment is 114°.
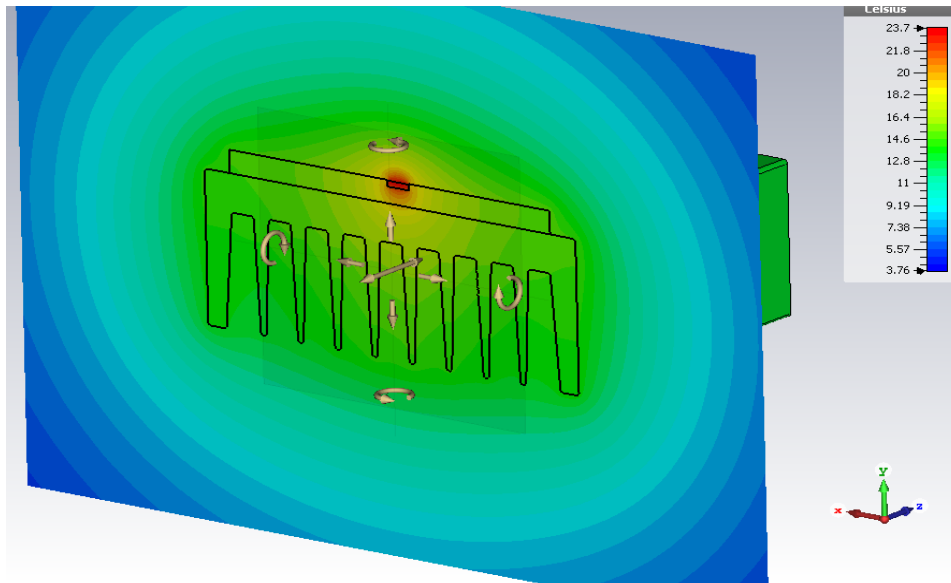


Figure 8: Temperature distribution in the heat sink-spreader structure at the steady state

For a transistor maximum temperature of 200 °C and by considering a safety margin of 20 °C, 50 W of dissipated power are tolerated for ambient temperature up to 66°C.

# V POWER AMPLIFIER DESIGN AND MEASUREMENTS

Fig. 9 shows the single ended amplifier schematic. The optimal load impedance for a 100 W amplifier with 48 V drain voltage is 12.5 Ω and this value is easily reached with the coaxial transformer previously described [11], [19]. In this design, the GX3442 transistor has been stabilized with an input series and parallel resistances of 12 Ω and 20 Ω, respectively.

A shunt capacitance of 47 pF has been added in parallel to the series resistance to improve the flatness of the amplifier gain. It is worth noting that the amplifier stability is strongly influenced by the transformer losses modeled with the RF resistors (see Fig. 5). This is confirmed by the results reported in Fig. 10 where the stability Rollet factor [1] for the amplifier with and without the RF resistors is reported. The figure shows that the presence of parasitic resistors makes the amplifier unconditionally stable over all the frequency bandwidth.

Fig. 11 shows the amplifier layout and Fig. 12 its realization over a RO4350B 30 mil substrate. It is important to note that, in order to respect the simulated thermal performances, care must be placed in a proper treatment of the spreader surface.
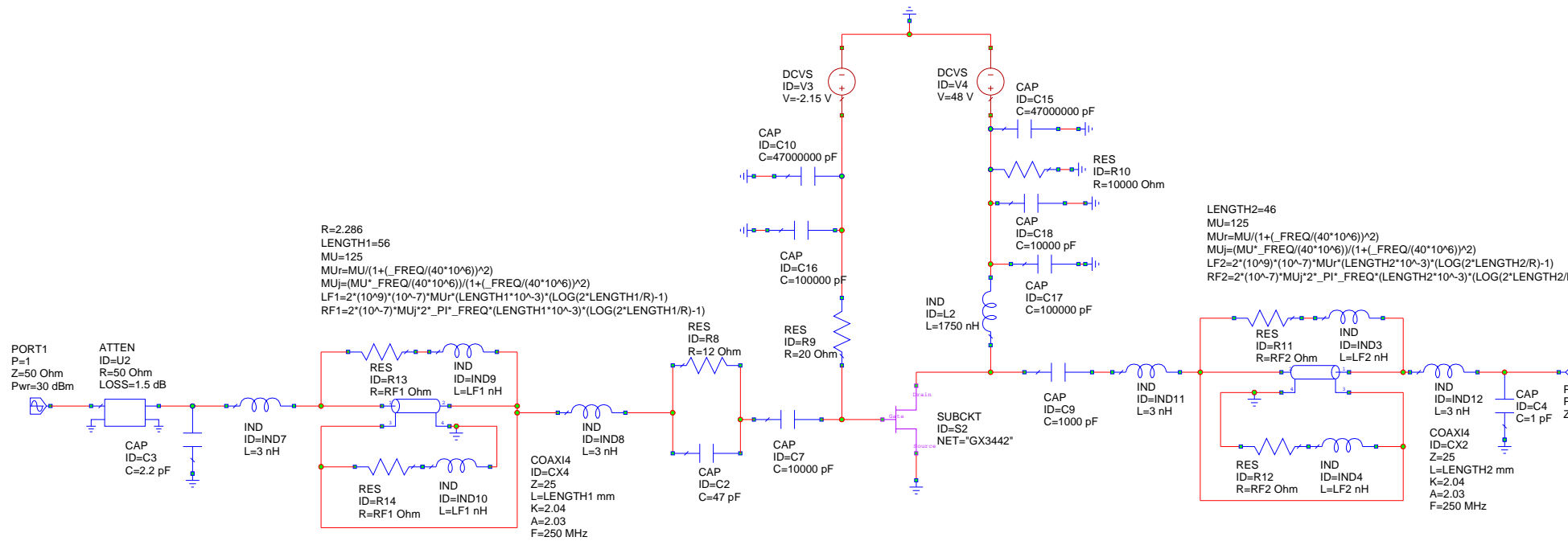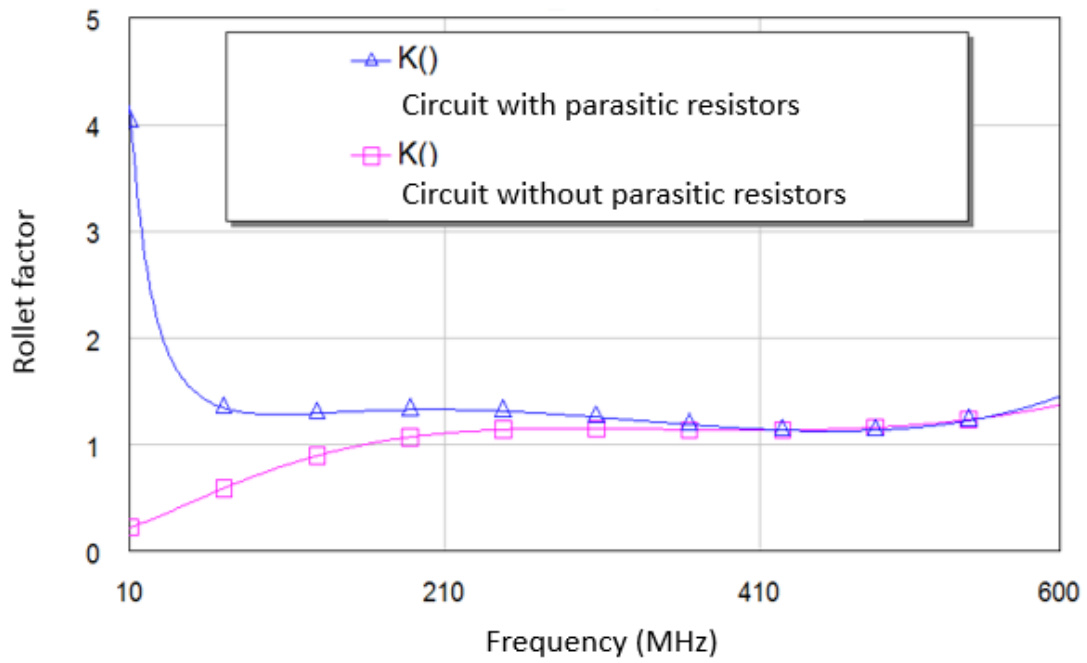
Figure 9: Amplifier schematic

Figure 10: Stability Rollet factor for the amplifier with and without the parasitic resistors
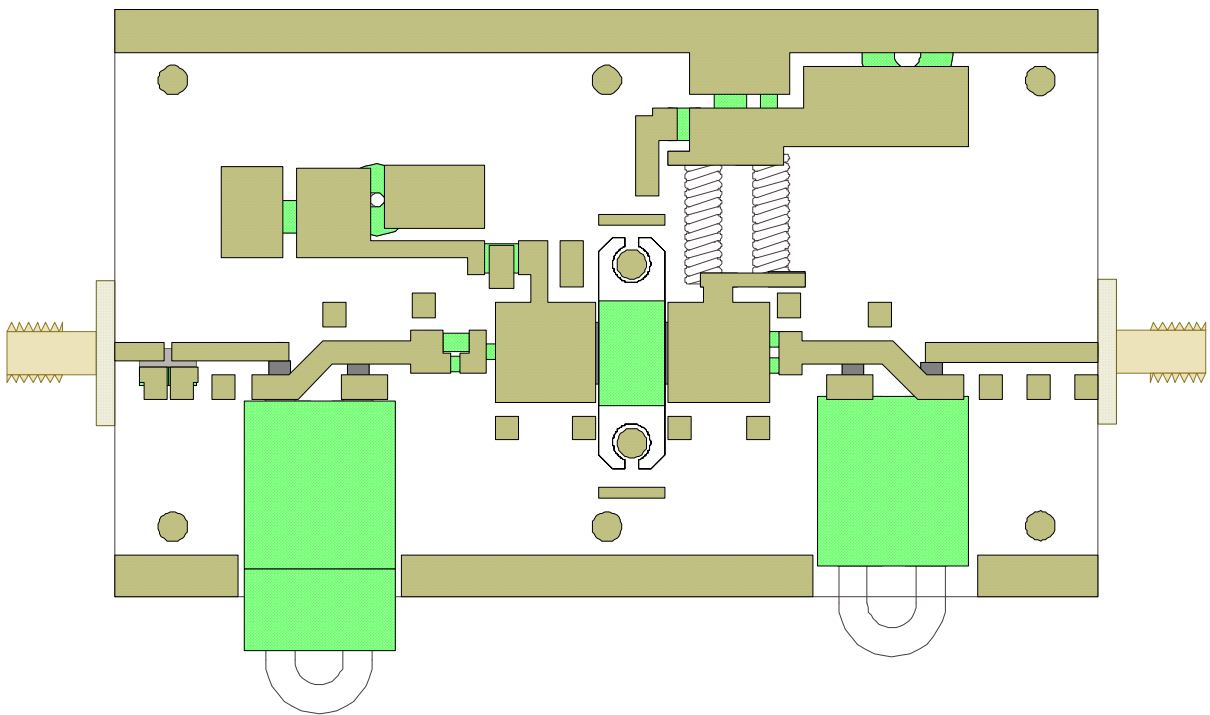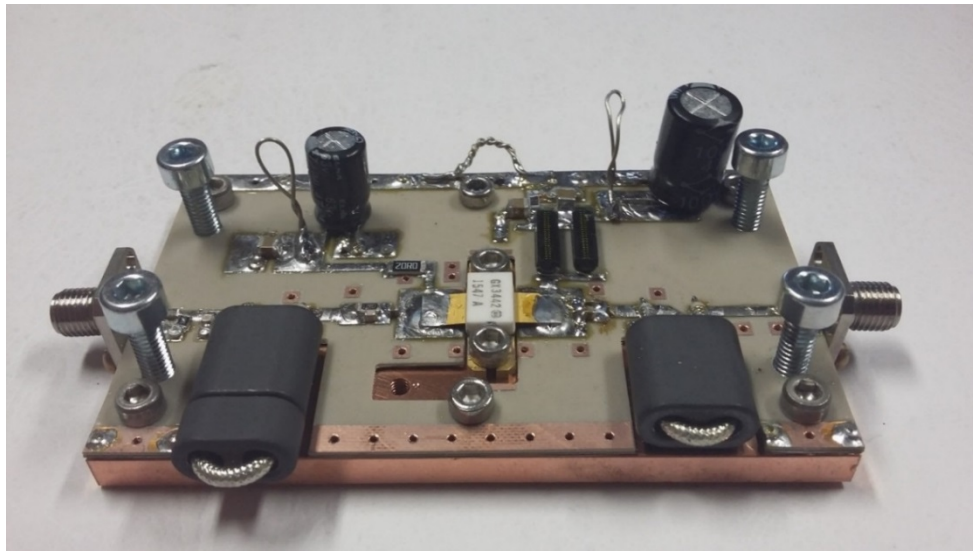


Figure 11: Amplifier layout

**(a)**



(b)

Figure 12: Amplifier realization: Top view (a) and lateral view (b)

Fig. 13 shows a comparison between the small signal scattering parameters simulated on the circuit of Fig. 9 and those measured with a PNA E8363B on the realized PA (see Fig. 12). A very good agreement between simulation and measurement is evidenced. In particular, the obtained agreement indicates that all the parasitic components of the structure have been properly taken into account.
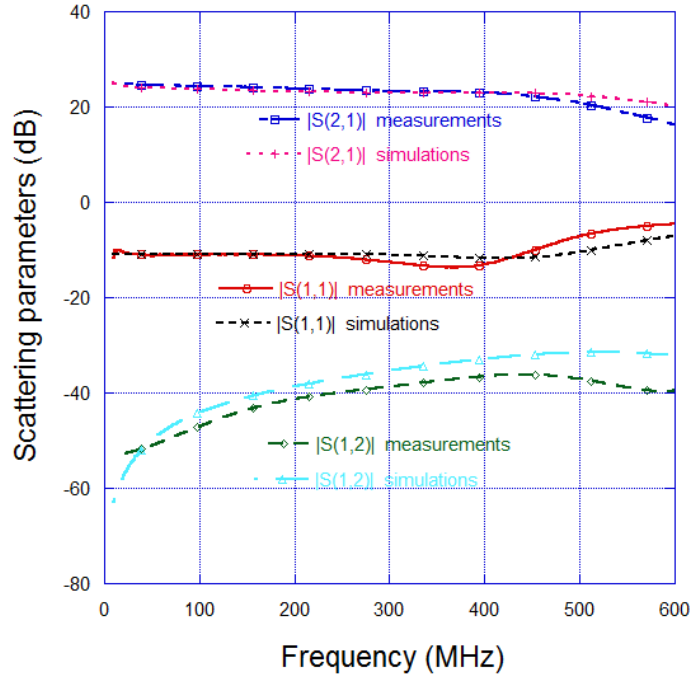
Figure 13: Comparison between simulated and measured small signal scattering
parameters

For high power measurements, the experimental set up depicted in Fig. 14 has been used. In the figure, together with the used components, the power budget is also reported.

Fig. 15 shows Gain, Return Loss and PAE of the amplifier evaluated for 30 dBm of input power. The measured gain is 19 dB +/- 1 dB, and the return loss is lower than -7.5 dB with a good agreement between measurement and simulations. Concerning the measured PAE, its average value is about 61% with 15% oscillations. The simulated average PAE (61% ± 7%) is similar to the measured one but with a different frequency behavior.

Finally, Fig. 16 shows the 2nd and 3rd order harmonic power with respect to the carrier for 30 dBm of input power. The figure shows that measurement exhibit the same frequency behavior of simulations with values comparable or a bit better.
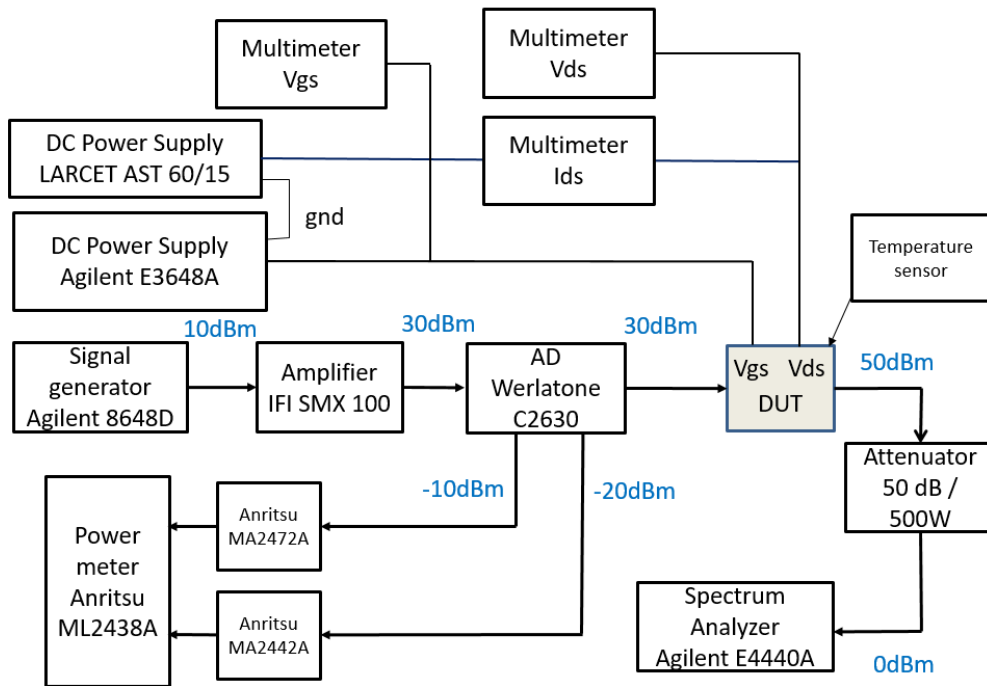
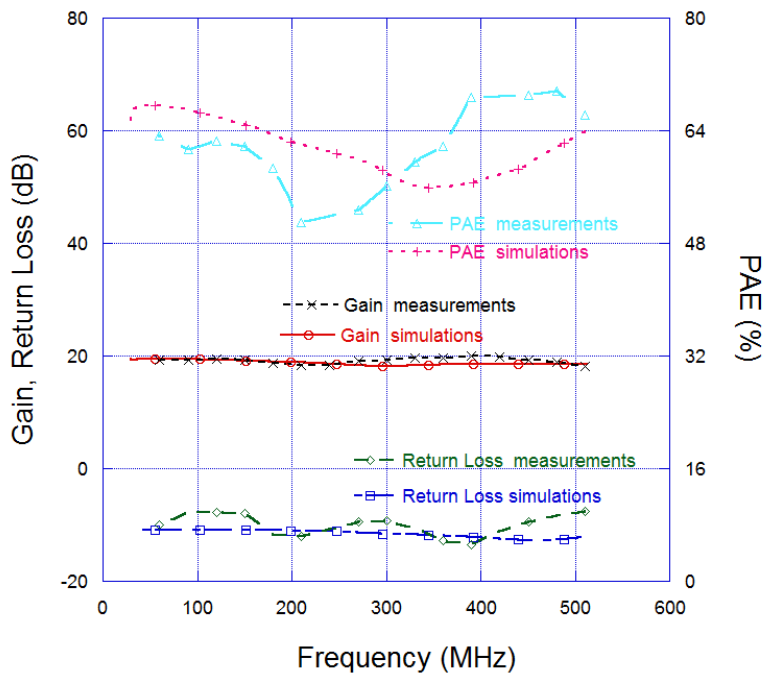Figure 14: Experimental set up used for high power measurements



Figure 15: Simulated and measured Gain, Return Loss, and PAE of the amplifier evaluated for 30 dBm of input power
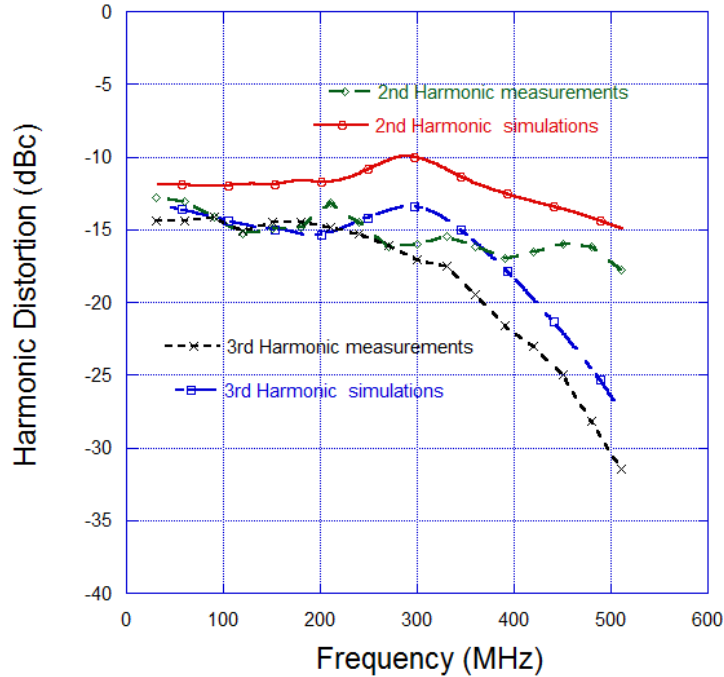
Figure 16: Simulated and measured 2$^{nd}$ and 3$^{rd}$ harmonics powers relative to the carrier for 30 dBm of input power

## VI CONCLUSIONS

A class AB single ended power amplifier with 30-512 MHz frequency band and 100 W saturated output power has been designed and built with Vds = 48 V and Idq = 400 mA. Simulations performed with the CAD microwave studio by CST have been employed to design the amplifier matching networks and the heat removal assembly.

The use of electromagnetic simulations has allowed to extract an accurate model of the matching coaxial transformer taking into account all the losses and parasitic elements. This model has been inserted in to the circuital CAD NI AWR allowing the optimization of the stability and matching networks.

With the aid of thermal simulations the spreader to heat sink and heat sink to air thermal resistances have been estimated and the maximum power that can be dissipated in the transistor as a function of the ambient temperature has been evaluated.

For 30 dBm input power, the measured gain was 19 dB +/- 1 dB, the average PAE was 61% and the return loss was always better than -7.5 dB. The measured responses were in good agreement with simulation results.

With respect to other kinds of HPAs operating in the 30-512 MHz band the proposed single ended GaN realization shows good performances in terms of Gain, Return Loss and PAE but higher values of harmonics. However, the non-linearity of the amplifier can be improved by combining two identical amplifiers in phase opposition or by using linearization techniques such as the feed-forward or the digital predistortion. So, the proposed amplifier can be efficiently used when linearity performance are not required but also as an useful device to test linearization techniques and algorithms.

## REFERENCES

1.  S.C. Cripps, "*RF power amplifiers for wireless communications*", Artech House, 2006.

2.  J.L.B. Walker "*Handbook of RF and Microwave Power Amplifiers*", Cambridge University Press, 2012.

3.  Electronic Communications Committee (ECC) within the European Conference of Postal and Telecommunications Administrations (CEPT), "The European table of frequency allocations and applications in the frequency range 8.3  kHz to 3000 GHz, approved May 2015.

4.  D. Vye et al, "*The new power brokers: high voltage RF devices*", Microwave Journal,

5.  S.M. Sze, K.K. Ng, "*Physics of Semiconductor Devices*", Wiley, 2006.

6.  A. Moore, J. Jimenez, "*GaN RF Technology for dummies*", Wiley, 2015.

7.  D. Xiao, D. Schreurs, C.V. Niekerk, W. De Raedt, J. Derluyn, M. Germain, B. Nauwelaers, G. Borghs, "Wide-band hybrid power amplifier design using GaN FETs," *Int. J. RF and Microwave CAE*, vol. 18, pp. 536-542, 2008.

8.  Polyfet rf devices: GX3442 datasheet, Sept. 2013.

9.  W. R. Curtice, "A MESFET model for use in the design of GaAs integrated circuits", *IEEE Trans Microwave Theory Tech* , vol. 28, pp. 448-456, May 1980.

10. Polyfet rf devices: application note TB255, Mil Comms GaN, simple layout, Jan. 2016.

11. C.G. Gentzler and S.K. Leong, "Broadband VHF/UHF amplifier design using coaxial transformer", *High Frequency Electronics*, pp. 42-51, May 2003.

12. A. Grebennikov, "Power combiners, impedance transformer and directional couplers," *High Frequency Electronics*, pp. 20-38, Dec 2007.

13. S. Lin, A.E. Fathy, G.M. Hegazi, T.T. Chu, "Circuit and EM modeling of wideband high power VHF/UHF combiners," *Int. J. RF and Microwave CAE*, vol. 19, pp. 481-491, 2009.

14. P. Debye, Polar Molecules, The Chemical Catalog Company, Inc., New York, 1929. Section 18, pp. 89-95.

15. Moran, Shapiro, Munson, DeWitt "Introduction to thermal systems engineering, thermodynamics, fluid mechanics, and heat transfer" Wiley, 2003.

16. Ellison "Thermal Computations for Electronics: Conductive, Radiative, and Convective Air Cooling" CRC Press, 2010

17. Yovanovich and co, "Four Decades of Research on Thermal Contact, Gap, and Joint Resistance in Microelectronics" *IEEE transactions on Components and Packaging technologies*, vol. 28, no. 2, June 2005

18. CST - Thermal Modeling of Heat Sinks – Online document

19. R. Baker, "*GaN solutions for next generation military communications*", Macom, 2014.